

Re-Analysis of Polarization in the γ -ray flux of GRB 021206

Robert E. Rutledge and Derek B. Fox¹

ABSTRACT

A previous analysis of the *Reuven Ramaty* High Energy Solar Spectroscopic Imager (*RHESSI*) observation of GRB 021206 found that the gamma-ray flux was $80 \pm 20\%$ polarized. We re-examine this data and find no signal that can be interpreted as due to polarization. First, we find that the number of scattering events suitable for measuring polarization – having been scattered from one detector to another, with a count produced in both – is considerably lower than estimated by CB03, by a factor of 10 (830 ± 150 , vs. 9840 ± 96). The signal-to-noise of the data-set is thus too low to produce a detection, even from a 100% polarized source. Nonetheless, we develop a polarization-detection analysis limited in sensitivity only by Poisson noise, which does not require a space-craft mass model to detect polarization, as in CB03. We find no signal which might be interpreted as due to polarization of GRB 021206. Separately, we reproduce the CB03 signal and show that it is not due to polarization. Rather, the CB03 signal is consistent with the previously-neglected systematic uncertainty in the “null lightcurve” used for detection. Due to the low signal-to-noise ratio of the *RHESSI* data, our Poisson noise-limited analysis results in an upper limit consistent with 100%-polarization of the gamma-ray flux from GRB 021206. Thus, no observational constraint on the polarization of GRB 021206 can be derived from these data.

1. Introduction

Gamma-ray bursts (GRBs) are associated with the deaths of massive stars, as seen first in their association with blue galaxies (Bloom et al. 1999; Bloom et al. 2002a); the appearance of supernovae explosion (SNe) -like lightcurves at late times (Bloom et al. 2002b); and the recent convincing observation of a SNe spectrum associated with a GRB afterglow (Hjorth et al. 2003; Stanek et al. 2003). However, what differentiates GRBs from the 10^4 more frequently observed core-collapse, or type-II, SNe remains uncertain.

¹Division of Physics, Mathematics and Astronomy; California Institute of Technology, MS 130-33, Pasadena, CA 91125; rutledge@tapir.caltech.edu, derekfox@astro.caltech.edu

Recently, it was reported (Coburn & Boggs 2003, CB03 hereafter) that $80\pm 20\%$ polarization in the prompt, or burst, gamma-rays of GRB021206 was detected using the Spectroscopic Imager (Smith et al. 2002) on board the *RHESSI* satellite (Lin et al. 2002). Although not designed for gamma-ray polarization measurements of GRBs, the multiple detectors of *RHESSI* were used to search for simultaneous events in two detectors due to Compton scattering, which then give a preferred scattering direction projected on the sky. An excess of scattered events in a particular direction on the sky was interpreted as due to angle-dependent scattering associated with intrinsic polarization of the gamma-ray photons.

Such a high polarization fraction in the gamma-rays may require a large-scale persistent magnetic field – of a strength observed thus far only from neutron stars, in particular the magnetars which are believed to account for $\lesssim 10\%$ of the observed NS population. If this property of GRBs is confirmed in future observations, then polarization would strongly constrain GRB production models, and may provide important input physics to understanding the generalized SNe phenomena. The reported detection has led to the wide discussion of mechanisms for producing the high polarization, which would constrain the emission and progenitor models (Lyutikov et al. 2003; Granot 2003; Eichler & Levinson 2003; Nakar et al. 2003; Lazzati et al. 2003; Matsumiya & Ioka 2003), and has prompted discussion of detector development to better observe gamma-ray polarization (Bloser et al. 2003).

The analysis of CB03 used a mass-model for the *RHESSI* satellite to calculate the satellite response to an unpolarized beam, in order to calculate the unpolarized lightcurve. It is first needed to calculate the "null" lightcurve (that is, the lightcurve of an unpolarized GRB) to demonstrate detection. It is also needed to correct the detected signal, and dominates the error bar in the measurement of $80\pm 20\%$ polarization.

We describe the observation in §1.1, and give an overview of the analysis by CB03 in §1.2. To produce the polarization measurement, it is necessary that photons scattered between two detectors be observed in the data, and in §2 we estimate the number of observed scattered double-count events, finding it to be a factor of 10 lower than the previous estimate. In §3, we examine the distribution of single counts and double counts as a function of the instantaneous position of the detectors where the counts are detected, and find that, while both single- and double- counts exhibit strong dependencies on this position, their ratio does not, suggesting the absence of a signal due to polarization. We nonetheless describe in §4 a polarization detection analysis suitable for *RHESSI* data which is limited in its sensitivity by Poisson statistics (that is, not dependent upon the space-craft mass model) and apply it to the observation of GRB 021206, deriving a correction which accounts for the angle-dependent Klein-Nishina cross section in §4.2. The results of the

polarization analysis are discussed in §4.3, finding no evidence for a signal which could be due to polarized gamma-ray photons from GRB 021206. In §5, we reproduce the modulation reported by CB03, finding that the reported signal is not observed using the new method, which does not rely upon the Monte Carlo radiative transfer through the *RHESSI* mass model. In §8 we summarize our results, compare them with those of CB03 and conclude.

1.1. Observation of GRB 021206 with *RHESSI*

The observation of GRB 021206 is described by CB03. We recount pertinent information. The *RHESSI* satellite is a gamma-ray imager primarily for solar observations using a rotation modulated collimator. It is in a low-Earth orbit, with its imaging (z) axis staring within a few arc-minutes of the solar center. The entire satellite rotates approximately around this z axis clockwise from north, with a period of ~ 4 seconds.

The *RHESSI* spectrometer detectors are an array of 9 separate, effectively identical detectors, each a cylinder roughly 7.1 cm diameter. Each detector is electronically separated into two segments (“front” and “rear”) which have slightly different photon energy responses. A diagram of the detectors and their orientation within the spacecraft detector plane is given in (McConnell et al. 2002). We give a similar diagram in Fig. 1, and the mass-model coordinate centers of the detectors in Table 1.

The approximate start time of GRB021206 measured with *RHESSI* was 2002-Dec-06 22:49:16 UT. The best gamma-ray localization of GRB021206 was found (Hurley et al. 2003) to be an error ellipse centered at R.A.=240.195 deg (16h00m46.8s), dec.=−9.710 deg (−09d42m36s)(J2000), with a major axis of 20.4′ and a minor axis of 0.53′, position angle of −18 deg (relative to the positive direction of declination). We adopt the position of a related radio transient (Frail 2003).

At the time of the transient, the solar location was about R.A.=16h53m20.15s, dec.=−22d32m47.7s. The GRB was localized at an angle $\theta_{\text{GRB}} = 45$ deg clockwise from N of the sun, and offset from the direction of solar center by 17.98 deg. Counts detected with the *RHESSI* spectrometer are timestamped with resolution of 2^{-20} s, or 1 binary micro-sec (μs); the detector segment; and photon energy.

1.2. Approach of CB03

We refer the reader to CB03 for details of the analysis used to detect the polarization signal. We describe the pertinent approach here.

A double-count scattering event takes place when a gamma-ray photon makes a single scatter off of detector i , producing a count in that detector, then leaving that detector to be partially or fully absorbed in a second detector j , producing a simultaneous count in detector j . A double-count coincidence event, which appears identical to a double-count scattering event, takes place when two unrelated photons produce simultaneous counts in two different detectors. A single-count event takes place when a single photon is fully or partially absorbed in a detector i , but is not followed by a detection in another detector within some period of time ΔT as measured by the on-board clock.

When a double-count event is registered, the position angle on the sky (θ) of the line joining the centers of the detector pair is determined. From this, a lightcurve of double count events as a function of θ was produced.

CB03 produced a null double-count event lightcurve to be subtracted from the observed lightcurve by Monte Carlo simulation (S. Boggs, W. Coburn, priv. comm.). They simulated $\sim 18,000,000$ photons propagating through the spacecraft from the direction of the GRB, to produce a library of double-event scatters between detectors.

Following this subtraction, a sinusoidal modulation in the difference lightcurve was found, which was significantly different from a constant value. Based on this sinusoidal residual, CB03 concluded that the incoming gamma-ray beam was polarized. Using the scattering fractions found with the GEANT mass model, the magnitude of the modulation was corrected to find the intrinsic polarization magnitude of $80 \pm 20\%$. The uncertainty is dominated by uncertainty in the GEANT mass model.

2. Proportion of Scattering Events and Backgrounds

To estimate the sensitivity of the *RHESSI* spectrometer to gamma-ray polarization, it is critical to establish the presence and estimate the number of two-detector scattering events in the data, and to minimize, and also estimate, the level of contaminating two-detector backgrounds.

It is possible to analyze the *RHESSI* data for evidence of a polarization signature without investigating these effects. In most but not all cases (see §6), double-count event backgrounds will dilute the angular modulation signal but will not generate an angularly-modulated signal of their own, and thus will not mimic the effects of genuine gamma-ray polarization. However, even when modulation can be detected in this fashion, estimating the number of two-detector scatters and associated backgrounds still allows a valuable consistency check of the analysis to be made. Moreover, converting a detection of

modulation to an estimate of the polarization signal strength requires an accurate estimate of the signal and background.

CB03 present estimates of the number of two-detector scatter events and backgrounds in their “Methods” section. They find 9840 ± 96 two-detector scatters, and estimate a background of 4488 ± 72 two-detector coincidences and 588 ± 24 “background scatter” events, for a total of 14916 double-count events detected. The meaning of the “background scatter” category is not defined but would seem to refer to scattering events attributable to background sources other than GRB 021206 itself. They also state that the number of two-detector scatter events is “roughly 10% of the total 0.15–2.0 MeV light-curve events,” and that this proportion is in agreement with the results from their Monte Carlo simulations; the nature and degree of this agreement is not quantified.

In this section we make a model-independent investigation of the fraction of two-detector scatter events in the *RHESSI* data for GRB 021206. In particular, we determine the number of two-detector events which are due to events of each of the following types: (a) scattered events, which produce two counts in two different detectors from a single scattered photon; (b) the coincident arrival of two unrelated photons in two different detectors; (c) scattered events, which produce two events in the same detector; and (d) events which take place in different detectors due to a detector effect. For the polarization measurement, events of type (a) permit measurement of polarization; type (b) is the irreducible background; and types (c) and (d) are background which, in principle, can be identified by their non-Poissonian nature and removed from the data.

2.1. Relative Timing Accuracy of *RHESSI* Detectors

As a first step, we examine the timing properties of *RHESSI* spectrometer data to establish an appropriate definition for selection of “simultaneous” events. We find that it is necessary to accept events within a time window of $5 \text{ b}\mu\text{s}$ to avoid discarding simultaneous events.

Fig. 2a is a histogram of wait times between timestamps of consecutive counts (ΔT); for a pure Poisson process – not the present case, because of the strong variations in the GRB mean count rate – this histogram will exhibit the classical exponential form. We observe a clear non-Poissonian excess near $\Delta T \approx 2 \text{ b}\mu\text{s}$, that is, at ΔT greater than zero. Since the light-travel time for $2 \text{ b}\mu\text{s}$ is 570 m, far larger than the separations between detectors, this cannot be a physical effect, but rather must be due to behavior of the detector electronics, with simultaneous events not receiving identical timestamps.

In Fig. 2b we have removed the 6732 event pairs which take place either simultaneously or consecutively (with no intervening counts) in the same detector; the front and rear segments of a detector are considered to be the same detector for these purposes. Note that double-count, same-detector events are not useful for polarization measurement. While these events are a significant fraction of those with $\Delta T \leq 5$, we still observe a non-Poissonian excess of counts at $\Delta T=1\text{--}4\text{ b}\mu\text{s}$; in addition, we can see non-Poissonian excesses at $\Delta T=8, 12, 16, 20, 24, 28$ and $32\text{ b}\mu\text{s}$ ². These excesses indicate that the spacecraft timestamps are subject to systematic uncertainties at the $\Delta T \sim 4\text{ b}\mu\text{s}$ level, and possibly even at the $32\text{ b}\mu\text{s}$ level. Thus, we treat event pairs with $\Delta T \leq 5\text{ b}\mu\text{s}$ as simultaneous in our subsequent analyses.

As a consequence of this definition, if we observe more than two consecutive counts within $5\text{ b}\mu\text{s}$ of each other, their simultaneity makes it impossible to extract a unique scattering event from the group. We therefore exclude all events within such multi-event groupings from our analysis.

2.2. Double-Count Events Due to Coincidence

To evaluate the degree to which the counts statistics are Poissonian, we bin the data into a lightcurve with time resolution $\Delta T=5\text{ b}\mu\text{s}$.

To account for the highly variable nature of the GRB light curve, we estimate the countrate in $\delta t = 0.005\text{ s}$ intervals, treating the count rate over each interval i as constant for purposes of estimating the Poissonian mean rate μ_i . For the entire selected portion of the GRB light curve, we find the number $N_{j,\text{obs}}$ of $5\text{ b}\mu\text{s}$ bins containing j counts to be $N_{0,\text{obs.}}=969787$, $N_{1,\text{obs.}}=72510$, $N_{2,\text{obs.}}=5666$, and $N_{>2,\text{obs.}}=481$ bins, respectively.

Estimating the Poisson mean rate $\mu_i = N_{1,\text{obs},i}/N_{0,\text{obs},i}$ in each interval from the number of single-event and zero-event time bins, we calculate the number of $5\text{ b}\mu\text{s}$ time bins within that interval that will contain 2 (N_2) or >2 ($N_{>2}$) events, respectively, due to Poisson fluctuations:

$$N_2 = \frac{\delta t}{\Delta T} \sum_i \frac{\mu_i^2}{2} e^{-\mu_i} \quad (1)$$

$$N_{>2} = \frac{\delta t}{\Delta T} \sum_i 1 - (1 + \mu_i + \frac{\mu_i^2}{2}) e^{-\mu_i} \quad (2)$$

²The excesses are even more apparent if one looks only at events detected in the rear segments. The origin of these excess counts at $4\text{ b}\mu\text{s}$ is related to a detector deadtime effect (D. Smith, priv. comm.)

Summing over all δt intervals, we find $N_2 = 3760 \pm 30$ bins. The remaining excess of $(5666 - 3760) = 1906 \pm 81$ double-event bins are not due to coincidence (event type b), and must be due to non-Poisson processes (event types a, c, or d).

A disproportionate fraction of these arise from double-count events within a single detector (event type c). Of the $N_{2,\text{obs}} = 5666$ events, 1313 are due to simultaneous events in the same detector, compared to the $1/9 \times 5666 \approx 630$ events expected from coincidence.

As a result, when we require the two events in each double-event bin to rise from different detectors, we find an observed number of $N_{2,\text{obs},\text{dd}} = 4983 \pm 83$ double-event, different-detector bins compared to an estimated number of $N_{2,\text{dd}} = 8/9 \times N_2 = 3342 \pm 27$ due to Poisson coincidence alone. This implies that 1641 ± 87 double-event, different-detector bins may be due to scattering or unidentified detector effects (event types a or d).

2.3. Double- and Multi-Count Events Due to an Unknown Process

While we find the number of bins with > 2 events due to coincidence is $N_{>2} = 159 \pm 2$ bins, we observe $N_{>2,\text{obs}} = 481$ bins, for an excess of 322 ± 22 bins, which must be due to non-Poisson processes (event types a, c or d).

If these non-Poisson events were due exclusively to scattering processes, then the number of double-count events will be a fraction f of single events $N_{2,\text{scattering}} = f N_1$, the number of triple scattering events $N_{3,\text{scattering}} = f^2 N_1$, and number of j - scattering events $N_{j,\text{scattering}} = f^{j-1} N_1$. Thus, the ratio $r = N_{2,\text{scattering}}/N_{>2,\text{scattering}} = 1./(\sum_{i=1} f^i)$. Taking $f = N_{2,\text{obs.}}/N_{1,\text{obs.}} = 1906/85387 = (2.2 \pm 0.1) \times 10^{-2}$, we find $r = 44 \pm 2$, while we observe $r_{\text{obs.}} = N_{2,\text{obs.}}/N_{>2,\text{obs.}} = 1906/322 = 5.9 \pm 0.5$ (here, we have not corrected for double-count events due to scatters within a detector)³.

Thus, there are a factor 7.8 ± 0.8 more $N_{>2,\text{obs.}}$ events relative to the number of N_2 events than can be explained by scattering events. We compared the distribution of detectors and photon energy for counts included among the observed $N_{>2}$ events, and found they do not differ significantly from the same distributions of all the GRB data. Specifically, the multi-count events typically occur in more than one detector.

We performed an identical analysis on data from during a background period

³The cross section for Compton scattering increases by a factor of ~ 2 between 1 MeV and 150 keV. In a worse-case, the $N_{3,\text{scattering}} = (2f)fN_1$ and $N_{N>2,\text{scattering}} = (2f)^{N-1}fN_1$, and $f = 22.7$ – still discrepant with the observations.

(43180 counts in 24 s), and found non-Poissonian $N_{>2}$ bins present in those data as well. The background period should have produced $N_{>2,\text{bg}} = 0.2$ bins (on average), but $N_{2,\text{bg,obs.}}=1013$. Also during this period, $N_{2,\text{bg}} = 105 \pm 1$, while $N_{2,\text{bg,obs.}}=3827$ bins were observed. Therefore, these non-Poissonian excess events are not associated with the GRB.

We attribute this non-Poissonian excess to an unknown process – perhaps particle background, or noise in the detector electronics or instrumentation – which we are unable to precisely model. Nonetheless, based on the background period, the non-Poisson process produces a ratio of counts $r_{\text{obs.},\text{bg}} = (3827 - 105)/(1013 - 0.2) = 3.7 \pm 0.1$, significantly below the value of 5.9 ± 0.5 observed during the burst.

It seems reasonable that the same unknown process can also produce double-count events, contributing to the double-count event background; however, the process is clearly non-Poissonian, and we are unable to produce a demonstrably reliable estimate of the number of such events⁴. Nonetheless, we note the effect and its uncertain contribution to the irreducible background as an event type d.

2.4. Summary of Corrections for Double-Count Event Rate

From analysis in this section, we conclude:

1. counts with time-tags different by $\leq 5 \text{ b}\mu\text{s}$ should be regarded as simultaneous;
2. double-count events within a single detector contribute significantly, adding to the background of double-count events, but are easily identified in the data stream, and should be replaced with a single count at the earlier time-stamp;
3. An unknown effect produces multi-count groups (> 2) of simultaneous counts in different detectors in excess of the number expected from coincidence, and which cannot be attributed to a scattering process, both during the GRB and during an earlier background period. These groups can be identified in the data-stream as occurring in a period $\leq 5\text{b}\mu\text{s}$; since they cannot be used for measuring polarization – as which two of the > 2 events were the sequentially first cannot be determined – these events should be removed prior to analysis;

⁴If, however, we assume that $r_{\text{obs.}}$ is constant between the background and the GRB observation, then the number of double-count events during the GRB which could be due to type a events is $1906 \pm 81 - 3.7 \pm 0.1 \times (322 \pm 22) = 715 \pm 120$ counts.

4. The same non-Poissonian, non-scattering effect likely also produces double-count events; we can estimate the number of double-count events based on the ratio $r_{\text{obs.}} = (N_{2,\text{obs.}} - N_2)/(N_{>2,\text{obs.}} - N_{>2})$ (correcting each value for the coincidence rate) observed during the background observation. However since we cannot model the non-Poissonian process which is responsible for this ratio, the ratio has an unquantifiable systematic uncertainty.

Based on this analysis, we sequentially apply the following selections to the GRB data to obtain double-count events using un-binned data:

- Replace all double-count events in the same detector with single-counts, at the earlier time stamp (83300 counts remaining afterwards). This removes “echo” counts in the detector (Smith 1998).
- Remove groups of >2 events which take place in ≤ 5 b μ s, ($N_{>2,\text{obs.}}=719$ such multi-count events, which is in excess of the $N_{>2}=474$ such events expected from Poisson statistics, leaving 81034 counts).

Following these selections, we have $N_{2,\text{obs.}}=8230$ double-count events remaining. This is fewer than the $N_{2,\text{obs.}} = 14916$ found by CB03. We list the contributions of “signal” and the irreducible background to these totals in Table 2.

To estimate the contribution to the irreducible background caused by coincidence of two unrelated photons in two different detectors, we use a similar approach as in § 2.2. We use an integration time of $\delta t = 0.005$ sec, and find the number of single counts which have another which follows within $\Delta T = 5$ b μ s. To do so, we calculate N_n , the number of unbinned events which are a collection of n counts within a period ΔT :

$$N_n = \sum_i \frac{\mu_i^{n-1}}{(n-1)!} \exp(-\mu_i) (N_i - (n-1))$$

where N_i is the number of detected counts in bin i , and $\mu_i = N_i \Delta T / \delta t$. Using this we find $N_2=6640 \pm 80$, after correcting by a factor 8/9 to account for the requirement that the counts be in two different detectors. This is greater than that found by CB03 ($N_2=4488 \pm 72$). If we were to assume a constant countrate throughout the burst we obtain $N_2 = 5380$ – lower than what we find for a variable intensity burst, but above that of CB03.

To estimate the contribution to the irreducible background due to the “unknown” process, we performed the same analysis as in §2.3, but to the

unbinned data, obtaining $r_{\text{obs.}}=3.1\pm0.1$ from the background period, giving us $N_{2,\text{bkg}} = r_{\text{obs.}} \times (N_{>2,\text{obs.}} - N_{>2}) = 3.1 \pm 0.1(719 - 474) = 760\pm110$ double-count events due to the unknown process (this value has an unquantifiable systematic uncertainty).

The result of this is that we find significantly fewer non-coincidence double-count events than found by CB03 (830 ± 150 double-count events, vs. 9840 ± 96 by CB03).

We use these single and double-count event lists for analyses in §2.5, §3 & §4.

2.5. A Simpler Method of Determining the Double-Count Event Rate due to Scattering Between Detectors

There is a method to estimate the fraction of double-count events which are due to scattering between detectors considerably more straightforward than attempting to identify all the backgrounds, as we do above.

First, we note that for each detector the total solid angle subtended by secondary detectors varies (see Fig. 1). In particular, the relative solid angle seen by the inner detectors (numbers 1, 2, and 7) is significantly larger than that seen by the outer detectors (numbers 3–6, 8, and 9), and if scattering events represent a significant fraction of the total then this should be reflected in the number of double-count events involving each detector.

For the analysis in this sub-section only, we exclude detector 2, due to its different electrical set-up. We calculate, for each detector, the total physical solid angle (Ω_i) subtended by the other seven detectors, except where the lines of sight to the other detectors are blocked by detector 2. We also examined the total number of single-counts in each detector I_i observed during the GRB – if all detectors were equally sensitive (including shadowing by the spacecraft), they should have equal values of I_i , but they do not, indicating different sensitivities during the GRB. We use I_i as a measure of the detector responses (see Table 1 for Ω_i and I_i ; note that we use the counts selected as described in §2.4).

We then determine $N_{2,\text{obs}}(i)$ – the number of double-count events in which one of the counts appears in detector i . We model this observed event rate with the function:

$$N_2(i) = N_{2,\text{tot}} \left(\frac{I_i \Omega_i}{\sum_j I_j \Omega_j} f + \frac{I_i}{\sum_j I_j} (1 - f) \right) \quad (3)$$

where $N_{2,\text{tot}}$ is held fixed at the observed number of counts for the double-events in detectors

1 and 3-9 (10906). Here, the coefficient on f is due to the scattered events involving two detectors. The coefficient on $1 - f$ is the random background. The value f can be measured because the values of Ω_i are different for different detectors. Our analysis ignores two effects: the angular dependence of the Klein-Nishina cross section for scattering, and the absorption/scattering effects of passive material between detector units, which will decrease the effective Ω_i by varying amounts, depending on the distance between detectors.

Using a χ^2 minimization fitting technique, we obtain an acceptable fit to the data ($\chi^2=9.28$ for 7 degrees of freedom – dof), for $f = 0.11 \pm 0.03$. The best fit and residuals, including the proportion of double events associated with scattering and coincidence, respectively, for each detector, are shown in Figure 4. Therefore, we find $11 \pm 3\%$ of the double-count events are due to scattering between detectors.

Comparing this with the value we found by attempting to eliminate all the reducible background sources we find $(11 \pm 3\% \times 8230 \pm 90 \text{ double-count events}) = 910 \pm 250$ double-count events due to scattering between detectors (where here use double-count events in all detectors, including detector 2). This is in agreement with the value of 830 ± 130 double-count events we found from the detailed analysis of the different background contributions.

3. Distribution of Observed Counts with Detector Angle

Fig. 5a presents the number of single counts S as a function of detector angle θ , where for each event θ indicates the position of the detector at the time of the event, relative to the center of the detector array in a non-rotating celestial frame ($\theta = 0$ is celestial north).

We see that there is a clear bias for single events to occur towards one side of the spacecraft. This could be due to a number of effects. For example, different detector sensitivities produce uneven exposure as a function of time over the range of θ which, combined with the GRB intensity variability (Fig. 3), can produce such a bias. Also, Earth-scattered gamma-rays – which may constitute a significant fraction of the total events – will preferentially illuminate the side of the spacecraft towards the Earth (see McConnell et al. 2002 for discussion).

The increased rate of single events towards one side of the spacecraft will produce an increased rate of double events on the same side through the increased coincidence rate (it will also produce an increased rate of double events through scattering). Fig. 5b presents the distribution $D(\theta)$ for the double events, where 2 values of θ are used (one for each detector involved in the double). $D(\theta)$ shows the same bias as the $S(\theta)$ distribution.

Indeed, the θ angular variations in the single and double count rates are highly correlated. This can be seen in Fig. 5c, which shows that although the χ^2_ν values for a constant fit to the variations of $S(\theta)$ and $D(\theta)$ separately are both very high (giving Prob. $< 10^{-50}$ in both cases), the χ^2_ν value for their ratio, $R(\theta) = D(\theta)/S(\theta)$, is close to unity, and acceptable for a constant fit (Prob. = 0.54).

If the double count events were due entirely to coincidences of independent single-count events we would expect that $D(\theta) \propto S(\theta)$. However, if a significant fraction of double-count events are due to scattering, and polarization of gamma-ray photons produces scatters toward a preferred direction in θ and $\theta + \pi$, as suggested by the results of CB03, then we should observe a $D(\theta)$ that was significantly different than $S(\theta)$. Our result here conflicts with this, suggesting instead that the variability observed by CB03 is not due to polarization-effected scattering, but due to systematic uncertainty in the calculation of their “null” lightcurve by MC simulation.

As a result, the coincidence rate for any given pair of detectors will increase when they are both on the preferred side of the spacecraft, and this may allow the derived “scatter angles” for the coincidence events to pick out a preferred direction on the sky. In the next section we describe and perform a polarization analysis which is insensitive to contamination from angular structure in the coincidence events, which is clearly the dominant effect in the observed double-count event variability.

4. A Mass-Model Independent Polarization Analysis

We describe in this and the following sections a method for detecting polarization which does not rely upon the mass model of *RHESSI*.

The observed countrate in a detector i is:

$$N_i(t) = f(t)A_i(t)$$

where $f(t)$ is the time dependent flux ($\text{erg cm}^{-2} \text{s}^{-1}$) and $A_i(t)$ is the detector response (counts erg^{-1}), which we allow to be time-dependent due to the rotation of *RHESSI* with respect to the sky. We assume that the probability that a count: (1) is a single-scattering event in detector i ; (2) escapes detector i ; and (3) is then partially or fully absorbed in a second detector j , is a time-independent factor $B_{i,j}$, dependent only on the materials and geometry of the *RHESSI* spectrometer.

The number of double-count events due to unpolarized photons between detectors

i and j at a time t when the centers of those two detectors produce a line which has a position angle $\theta_{i,j}$ on the sky (relative to the north celestial pole) can be found:

$$N_{i,j}(t) = N_i(t)B_{i,j} + N_j(t)B_{j,i} \quad (4)$$

If the beam is polarized, this produces a polarization pattern $I_p(\theta_{i,j})$ where $\theta_{i,j}(t) = \omega t + \phi_{i,j}$ is now the angle the detectors make on the sky as a function of time, and ω is the rotational frequency of the *RHESSI* detector plane, and $\phi_{i,j}$ is the angle the detector pair (i, j) makes on the sky at time $t = 0$.⁵

$$N_{i,j}(\theta_{i,j}(t)) = N_i(\theta_{i,j}(t)) I_p(\theta_{i,j}) B_{i,j} + N_j(\theta_{i,j}(t)) I_p(\theta_{j,i}) B_{j,i} \quad (5)$$

where we use the polarization intensity pattern:

$$I_p(\theta) = \frac{1 + p \cos(2(\theta - \theta_p))}{1 + p} \quad (6)$$

(This differs by $\pi/2$ from a different, oft-used definition). Now, $I(\theta_{i,j}) = I(\pi + \theta_{i,j}) = I(\theta_{j,i})$; and $B_{i,j} = B_{j,i}$ for the identical detector geometries which are used by *RHESSI*. Thus:

$$N_{i,j}(\theta_{i,j}) = [N_i(\theta_{i,j}(t)) + N_j(\theta_{i,j}(t))] B_{i,j} I_p(\theta_{i,j}) \quad (7)$$

Each side of this equation can be summed over all detector combinations, keeping data binned as a function of θ ; then

$$\sum_{i,j>i}^{\theta<\theta_{i,j}<\theta+\Delta\theta} N_{i,j}(\theta_{i,j}) = I_p(\theta_{i,j}) \sum_{i,j>i}^{\theta<\theta_{i,j}<\theta+\Delta\theta} [N_i(\theta_{i,j}(t)) + N_j(\theta_{i,j}(t))] B_{i,j} \quad (8)$$

which we can then re-write as a ratio, which is a function of sky-angle only:

$$R(\theta) = \frac{\sum_{i,j>i}^{\theta<\theta_{i,j}<\theta+\Delta\theta} N_{i,j}(\theta_{i,j})}{\sum_{i,j>i}^{\theta<\theta_{i,j}<\theta+\Delta\theta} (N_i(\theta_{i,j}) + N_j(\theta_{i,j}))} \quad (9)$$

⁵We do not correct the polarization angle measured at the detector, which is projected relative to the North Celestial Pole, to the angle relative to the north from the GRB position in the sky. The difference varies as a function of polarization angle by up to 3 deg systematically. This is <20% of our 15 deg bins, and will not affect our conclusions.

$$= C \frac{1 + p \cos(2(\theta - \theta_p))}{1 + p} \quad (10)$$

If $p = 0$ (unpolarized photons) then $R(\theta)$ is a constant, with no dependence on θ . However, if $p \neq 0$, then the observed function $R(\theta)$ will have an angular dependence, as $I_p(\theta)$.

The only contribution to the uncertainty in $R(\theta)$ is photon counting statistics. More specifically, $R(\theta)$ is independent of the mass model of the spacecraft, and the uncertainty of detection of polarization using $R(\theta)$ does not depend on systematic uncertainties in the space-craft mass model as it does in CB03. However, it should be noted that correcting a detected signal to find the intrinsic polarization magnitude (that is, turning the detection into a quantitative measurement) would still require using the mass-model.

In practice, the function $R(\theta)$ is constructed from a discrete sum of double-count events and a discrete sum of single-event counts, as we describe in the following subsection.

Here, we note an additional correction. As discussed in §2.5, the total number of single events observed during the GRB I_i varies with detector i , which implies different sensitivities to events. If we take the relative sensitivity $f_i = I_i / \langle I_i \rangle$ to be independent of the detector geometry (which are assumed identical), then Eq. 4 becomes:

$$N_{i,j}(t) = N_i(t) f_j B_{i,j} + N_j(t) f_i B_{j,i} \quad (11)$$

Here and above, $B_{i,j}$ is a relative solid angle subtended by detector j from detector i . This correction affects Eq. 9, which becomes:

$$R(\theta) = \frac{\sum_{i,j>i}^{\theta<\theta_{i,j}<\theta+\Delta\theta} N_{i,j}(\theta_{i,j})}{\sum_{i,j>i}^{\theta<\theta_{i,j}<\theta+\Delta\theta} (N_i(\theta_{i,j}) f_j + N_j(\theta_{i,j}) f_i)} \quad (12)$$

4.1. Data Analysis for GRB 021206

We downloaded data from the public *RHESSI* archive⁶, which also makes available data analysis software we used – the Solar SoftWare (SSW) system written in IDL. We extract counts from photons with energy between 0.15 and 2 MeV during the observation

⁶<http://hesperia.gsfc.nasa.gov>

of the GRB roughly corresponding in time to those analysed by CB03 (see Fig. 3). We find 85387 such counts in the 5.0 sec interval we analyze, chosen to coincide with that analysed by CB03.

The background number of counts, measured during an earlier observational period, is 8636 ± 42 counts during the 5.0 second period.

We find 8230 double-count events (§2.4). To perform the analysis, we use a discrete summation for the lightcurve. To construct the 36 independent double-event light-curves $N_{i,j}(\theta_{i,j})$, we take:

$$\theta_{i,j}(t_k) = (\omega t_k + \phi_{i,j}) \bmod (\pi) \quad (13)$$

where t_k is the time of the earliest time-stamp of each double-count event. The values of $\phi_{i,j}$ are relative angles of the line joining the centers of detectors i and j , and the centers of detectors 1 and 2, except for $\phi_{1,2}$, which we set equal to the angle on the sky at time $t = 0$ clockwise of N made by the center-line joining detectors 1 and 2, and $\omega = 2\pi/(4.09 \text{ s})$ (the rotational frequency of the spacecraft at the time of the observation).

The angles $\phi_{i,j}$ were found using the coordinate positions for each detector as listed in Table 1. We divide the 180 degree range into 12 equal non-overlapping segments, beginning with $\theta_n = n \times 15 \text{ deg}$, with $n = [0, 11]$. We produce the summed double-event lightcurve dependent upon sky angle $D(\theta_n)$:

$$D(\theta_n) = \sum_k N_{i,j}(\theta_{i,j}(t_k))$$

Where $N_{i,j}$ takes the value of 1, for a double-event involving detectors i and j with time-stamp t_k . The angles are binned as $\theta_n < \theta_{i,j} < \theta_n + \delta_\theta$.

Thus, for each double-event at time t_k involving detectors i and j , we calculate the angle on the sky from Eq. 13, and add a count to the appropriate θ bin. This is shown in Fig. 5e.

We then construct the denominator from the single-event light curve:

$$S(\theta_n) = \sum_k \sum_{i_k, j! = i_k} f_j N_{i_k}(\theta_{i_k,j}(t_k))$$

where N_{i_k} takes the value of 1, f_j is described in §4, and for every event k in detector i_k ,

we calculate the angle on the sky for every detector pair which includes i_k ⁷. Thus, for each count k , detected at time t_k in detector i_k we find the eight angles on the sky $\theta_{i_k,j}$ produced by the i_k and j th detector, and add one count in each of the eight bins, including angle bins in which the same count falls more than once due to co-aligned detector pairs (such as detector pair 4 & 7 and pair 4 & 3). This is shown in Fig. 5d.

We produce $R(\theta_n) = D(\theta_n)/S(\theta_n)$, which is shown in Fig. 5f. We discuss this Figure in detail in §4.3, after first discussing the effect of the Klein-Nishina cross section on the detection in §4.2.

The uncertainty in $R(\theta_n)$ is set by the photon counting statistics of D and S . As a minor correction, it is the number of *unique* counts in each bin of S which contributes to the fractional uncertainty of S . Thus, if there are 40000 counts in a particular angle bin of S , but only 30000 of those are unique, then the contribution to the fractional uncertainty of $R(\theta)$ is $1./\sqrt{30000}$. Even so, the uncertainty is dominated by the smaller number of double-event counts, which are in the range 610-770 in each bin.

4.2. Effect of the Klein-Nishina Cross Section

The GRB was offset from the pointing axis, which is perpendicular to the plane of detectors, by 17.98 deg. Assuming a thin detector plane⁸, photons which first scatter in a detector on the side of the detector plane toward the GRB can scatter through an angle (to the second detector) of up to $\theta_{\text{KN}}=90 \text{ deg}+18 \text{ deg}=108 \text{ deg}$; while photons which first scatter on the side of the detector plane away from the GRB could scatter through an angle of up to $\theta_{\text{KN}}=90-18=72 \text{ deg}$.

The difference in scattering geometry produces a varying scattering cross section for gamma-rays in the 0.15-2.0 MeV energy range, dependent on θ – the angle between a line connecting the centers of the two detectors and the projection of the direction of the GRB from the optical axis in the detector plane – through the Klein-Nishina cross section:

$$\frac{d\sigma}{d\Omega}(\theta_{\text{KN}}) \propto \left(\frac{k'}{k}\right)^2 \left(\frac{k}{k'} + \frac{k'}{k} - \sin^2 \theta_{\text{KN}}\right) \quad (14)$$

⁷We note that using $f_i = 1$ instead of the relative apparent counts sensitivity, as if only the physical apparent cross sections $B_{i,j}$ were important, does not change our conclusions.

⁸In fact, the detectors are 8 cm long, comparable to their width and separation. We neglect this width throughout the analysis.

$$\frac{k'}{k} = \frac{1}{1 + \frac{h\nu}{m_e c^2} (1 - \cos \theta_{\text{KN}})} \quad (15)$$

$$(16)$$

This will produce directionally preferential scattering from a non-polarized beam of gamma-rays in the detectors. If the direction of the GRB is $\vec{k} = \sin \phi \hat{x} + \cos \phi \hat{z}$ (where ϕ is 18 deg) the line which joins two detectors as $\vec{r} = \cos \omega t \hat{x} + \sin \omega t \hat{y}$, then $\gamma(t) = \omega t$ and $\theta_{\text{KN}}(t) = \arccos(\sin \phi \cos \omega t)$.

In Fig. 6a, we plot the KN cross section as a function of γ , for $\phi = 18$ deg, and for four photon energies ranging from 0.15-2.0 MeV, normalized to its maximum value. The cross section changes by 20% for photons of energy 0.15 MeV, and by 35% for photons of energy 2.0 MeV as a detector pair rotates in the detector plane.

A non-polarized gamma-ray beam will produce an angle-dependent double-event count-rate in the *RHESSI* detectors proportional to the sum of the cross section in two detectors separated by 180 deg:

$$I_{\text{KN}}(\gamma) \propto \frac{d\sigma}{d\Omega}(\theta_{\text{KN}}) + \frac{d\sigma}{d\Omega}(\theta_{\text{KN}} + \pi) \quad (17)$$

We show $I_{\text{KN}}(\gamma)$ in Fig. 6b. The KN cross section results in an angle-dependent variation in total intensity of 7-9% across the 0.15-2.0 MeV band. For comparison, we include in this figure $I_p(\theta)$, for $p = 0.045$. To within our observational uncertainties, the KN cross-section can always be represented by $I_p(\theta)$ ⁹. It is notable that the KN cross-section produces an effect on the observed signal which is nearly identical to that expected from an intrinsically polarized beam.

The magnitude of “apparent polarization” (that is, the value of p which parameterizes $I_{\text{KN}}(\theta)$ using $I_p(\theta)$; see Fig. 6c) varies as a function of photon energy; it is $p = 5\%$ (for photon energy 0.15 MeV), increasing to 5.1% (near 0.30 MeV) and decreasing to 3.7% at 2 MeV.

This effect is easy to correct for during data analysis, if one knows the direction of the GRB relative to the detector pairs.

We calculated the fractional magnitude and direction of the KN effect on the double-count scattering events, by averaging the magnitude of the effect at the energy of

⁹While the $I_{\text{KN}}(\theta)$ is not identically parameterizable by $I_p(\theta)$ we find that parameters to $I_p(\theta)$ can typically be found which duplicates $I_{\text{KN}}(\theta)$ to better than 1% for $p < 0.1$.

each detected count during the GRB (neglecting the 10% of counts due to background) and finding the average and standard deviation, which were $\langle p_{\text{KN}} \rangle = 0.049 \pm 0.003$. We can represent the effect of the KN cross section on the intensity pattern produced by the GRB by:

$$I_{\text{KN}} = \frac{1 + 0.049 \cos(2(\theta - \theta_{\text{GRB}}))}{1.049}$$

where θ_{GRB} is the direction of the GRB projected onto the detector plane ($\theta_{\text{GRB}} = 45 \text{ deg E of N}$).

In the present data, the magnitude of p_{KN} will be decreased by a factor $I_{2,\text{scattered}}/I_{2,\text{observed}} (< 0.046)$ (90% confidence). Thus, in the present data, $\langle p_{\text{KN}} \rangle < 0.0022$, which, as we show in §4.3, is well below the detection limit.

Moreover, the magnitude of this signal is overestimated, as we have assumed infinitely thin detectors. The effect of finite sized detectors is to diminish the magnitude of this effect, as can be immediately seen, for example, in the limit of infinitely long detectors. Moreover, the need for the correction in the present work is absent; the maximum magnitude of the effect is $0.049 \times 830 \pm 150 = 41 \pm 7$ counts – smaller than the Poisson noise of the total double-count events (which is $\sqrt{8230} = 91$ counts). Thus, this effect will not be important in the present analysis.

4.3. Results

In Fig. 5f, we show $R(\theta)$ for the observation of GRB 021206. First, $R(\theta)$ is consistent with being a constant (reduced chi-squared value $\chi^2_\nu = 1.35$ for 11 dof). We therefore find no evidence of a signal which might be interpreted as due to polarization in the *RHESSI* data for GRB 021206.

To obtain a limit on a signal which might be interpreted as due to polarization, we find a best-fit for $I_p(\theta)$ ($\chi^2_\nu = 1.36$, 9 dof) with $p \leq 0.041$, or $\leq 4.1\%$ (90% confidence), finding a (likely, local) minimum at $\theta_p = 74 \pm 22 \text{ deg}$. A similar limit on p_{KN} is obtained holding fixed $\theta_{\text{GRB}} = 45 \text{ deg}$, ($p_{\text{KN}} < 0.04$), which is consistent with our calculated upper-limit for this effect.

5. Duplication of CB03 Results

We attempt to duplicate the results of CB03. In particular, we are interested in duplicating their observed double-event lightcurve. While the methods of producing the double-event lightcurve of CB03 have not been described as of this writing, there are only a few variables which were not specified by CB03: (1) ΔT ; (2) whether or not multiple-scattering events (“bunches”) are retained; and (3) the zero point for θ .

We show the raw (double-event) counts and residual counts as a function of θ ($D(\theta)$ hereafter) obtained by CB03 in Fig. 7a. The residual counts lightcurve is the difference between the raw counts and their MC estimation for the double-event count rate ($M(\theta)=D(\theta)-D_{\text{null}}(\theta)$), assuming zero intrinsic polarization, and using the GEANT mass model for radiative transfer through *RHESSI*¹⁰. We note that the average values of $D(\theta)$ and $D_{\text{null}}(\theta)$ found by CB03 coincide within $<0.1\%$.

We obtain a good duplication of the CB03 double-event count curves, using $\delta T=8$ b μ s (as compared with $\Delta T=5$ b μ s in our previous analysis); retaining all multi-count events (“bunches”, including triples and higher); and setting $\theta = 0$ to coincide with 12.6 deg E of N in the Ecliptic (Fig. 7b, top panel). Here, we find $N_2=15540$ counts, which is close to the $N_2=14916$ found by CB03. We rescaled the $D_{\text{null}}(\theta)$ calculated by CB03 so that $\langle D_{\text{null}}(\theta) \rangle = \langle D(\theta) \rangle$. The residual counts ($D(\theta)-D_{\text{null}}(\theta)$; Fig. 7b, bottom panel) is similar to that obtained by CB03 (Fig. 7a, bottom panel).

Using these same selections, we apply our $R(\theta)$ analysis. If the modulation seen in Fig. 7b (bottom panel) is due to polarization, we expect to see the a sinusoidal modulation in $R(\theta)$, too (see Eqns. 9 & 12). Instead (Fig. 7c), we see that $R(\theta)$ is scattered, significantly different from a constant ($\chi^2_{\nu}=2.49/11$ dof; prob.=0.4%), but with no systematic trend approximating a sinusoidal modulation. The scatter in $R(\theta)$ cannot be due to a constant polarization signal as implied by CB03 (as we presently show, the scatter is due to the “bunches”). We conclude from this that the signal observed by CB03 is not due to polarization in GRB 021206.

We then dropped from the analysis all the “bunches” of counts (multiplicities of 3 and greater). We do this, because we see no reason that polarized photons should be preferentially detected in events which involve ≥ 2 scatters. Moreover, as we have shown above, the bunches do not follow a Poisson distribution, and do not follow a

¹⁰It was this MC simulation which gave the estimate of $\Pi = 0.19 \pm 0.04$ – that of all photons which are detected as double-count events, $19 \pm 4\%$ have not been scattered previously in spacecraft passive material, and thus have the polarization intact during measurement.

simplistic distribution expected from scattering; we therefore interpret these “bunches” as a background signal. There were a total of 1272 such bunches, producing a total of 4592 double-count counts; after removal, there were 10948 double-count events remaining. We performed the analysis again: $D(\theta)$ and $D_{\text{null}}(\theta)$ in Fig. 7d, top panel; with residual counts $D(\theta) - D_{\text{null}}(\theta)$ in the bottom panel. While the modulation of the residual counts is reduced, there remains a significant deviation (in the range $\theta=100$ -180 deg).

However, the corresponding $R(\theta)$ (Fig. 7e) is consistent with a constant value ($\chi^2_{\nu}=0.66$, 11 dof, prob.=77%). Applying the identical analysis as above, we again obtain a limit of $p < 0.041$ (90% confidence). This means that polarization is not detected (and that the scatter in $R(\theta)$ in Fig. 7c is due to the presence of the “bunches” of counts).

When we duplicate the analysis of Sec. 2.5 on the data in Fig. 7b and c, we obtain a fraction of counts which may be due to double-count scattering events of $f=9\pm2\%$ ($\chi^2_{\nu}=6.0$, 6 dof; Prob.= 3×10^{-6}) and $8\pm3\%$ ($\chi^2_{\nu}=13.9$, 6 dof; Prob.=0.03), respectively. The fact that data which includes the “bunches” is not well-modeled by our scattering model is consistent with the conclusion that these events are not related to scattering.

To what can the modulation reported in CB03 be due? Since the lack of modulation in $R(\theta)$ implies that $D(\theta) \propto S(\theta)$, yet $D(\theta) - D_{\text{null}}(\theta)$ is not constant in θ , the modulation must be in $D_{\text{null}}(\theta)$, and not in $D(\theta)$. We attribute, therefore, the modulation observed by CB03 to neglected systematic uncertainty in $D_{\text{null}}(\theta)$, which we explore in § 7.

6. The Intrinsic Polarization of GRB 021206

Our parameter p is not the intrinsic fractional polarization Π of GRB 021206. The relationship of our parameter p to Π is:

$$p = \mu \Pi \frac{S}{S + B} \quad (18)$$

where Π is the intrinsic fractional polarization of GRB 021206; μ is the fraction of *RHESSI*-detected double-count photons which have not been previously scattered within the detector; S is the number of double-count events due to scattering, and B is the number of background double-count events (that is, not due to scattering).

If our parameter p is consistent with zero, then the intrinsic polarization Π is also consistent with zero; thus, regardless of the magnitude of (and uncertainties in) μ , S and B , our upper-limit of $p < 0.041$ implies a non-detection of polarization in the *RHESSI* data of GRB 021206. This is in conflict with the claim of detection described by CB03.

We now describe the origin of the discrepancy between these two results.

Based on our limit $p < 0.041$, $S = 830 \pm 150$ counts, and $S + B = 8230$ counts, we find the 90% confidence upper-limit for intrinsic polarization in GRB 021206 is $\Pi < 0.41/\mu$.

CB03 finds $\mu = 0.19 \pm 0.04$ from their Monte Carlo mass-model simulations, which we adopt. Relying upon this value, $\Pi < 2.14$ (fractional polarization, or $< 214\%$) – that is, an upper-limit which permits up to 100% intrinsic polarization for GRB 021206, implying that the observation is not sensitive to intrinsic polarization in GRB 021206.

The lack of sensitivity is due to the lack of double-count events from scattering; the number we found (830 ± 150 counts) is smaller than and in conflict with the number found by CB03 (9840 ± 96).

If we had found the fraction f of total double-count events from scattering to be that found by CB03 ($f = 66 \pm 1\%$; see Table 2), we would instead conclude that $\Pi < 0.46$ (90% confidence), compared with the $\Pi = 0.80 \pm 0.20$ (CB03). However, our analysis (§2.4) finds that $f = 11 \pm 3\%$, which produces instead a limit on the intrinsic polarization of GRB 021206 well above 100%.

Our conclusion is that the *RHESSI* dataset is not capable of detecting polarization in GRB 021206, due to the low signal-to-noise of the dataset (that is, a relatively small number of double-count scattering events compared to that estimated by CB03).

7. Systematic Uncertainty in CB03

In our analysis, the uncertainty in polarization *detection* is due only to Poisson noise (in $R(\theta)$); in the analysis of CB03, the uncertainty in polarization *detection* ($M(\theta) = D(\theta) - D_{\text{null}}(\theta)$) is the sum of Poisson noise and the systematic uncertainty in $D_{\text{null}}(\theta)$. CB03 neglect the systematic uncertainty in $D_{\text{null}}(\theta)$. Here, we show that this systematic uncertainty is not negligible.

The observable modulation lightcurve is:

$$M(\theta) = D(\theta) - D_{\text{null}}(\theta).$$

The systematic uncertainty in $M(\theta)$ due to radiative transfer through the spacecraft mass model appears in $D_{\text{null}}(\theta)$. In a simple formulation, one can represent this as:

$$D_{\text{null}}(\theta) = \langle D_{\text{null}}(\theta) \rangle \frac{\mu(\theta)}{\langle \mu \rangle}$$

The function $\mu(\theta)$ and its uncertainty was not given by CB03. To be able to neglect the systematic uncertainty in μ , its magnitude would need to be \lesssim half the Poisson uncertainty – $\lesssim 20$ counts, or 1.6% per angular bin, given the $\langle D(\theta) \rangle = 1250$ counts/bin.

We can estimate the uncertainty in $\mu(\theta)$ in the analysis of CB03 from the uncertainty in its mean value ($\langle \mu \rangle = \mu = 0.19 \pm 0.04$), which has a 25% uncertainty. If we take the uncertainty in $D_{\text{null}}(\theta)$ to be the same fractional value as the uncertainty in the average μ (25% per angular bin), we find approximately $\sigma_{\text{systematic}} \approx 0.25 \times 1250 (\text{counts/bin}) \approx 310$ counts/bin, much larger than the 20 counts limit, and which should appear directly in their difference lightcurve (their Fig.2, or our Fig. 7a)¹¹. However, their analysis shows only the Poisson uncertainty ($\sigma_{\text{Poisson}} \sim 40$ counts). Moreover, the neglected $\sigma_{\text{systematic}} = 310$ counts/bin is greater than the reported modulation magnitude (~ 120 counts/bin); thus, we see no reason to neglect it.

We conclude that the analysis for detection of polarization by CB03 incorrectly neglected the dominant uncertainty – the systematic uncertainty $D_{\text{null}}(\theta)$, which must be added in quadrature with the Poisson uncertainty. This uncertainty, from the above approximate analysis, is greater than the reported signal interpreted as due to polarization.

8. Discussion and Conclusions

In selecting data to analyze, we found 8230 double-count events (including signal and irreducible background). This is well below the 14916 double-count events found by CB03 (Table 2). The discrepancy appears to be due to two selections employed by CB03: (1) an unjustifiably wide time window for “simultaneous” events ($\Delta T = 8 \mu\text{s}$, whereas we see only $\Delta T = 5 \mu\text{s}$ as being justified) and (2) the inclusion of multi-count events (“bunches”), in which >2 counts are detected within ΔT .

We described an analysis to detect polarization in *RHESSI* data. We apply this analysis to the data for GRB 021206, and find no evidence for a signal which might be interpreted as due to polarization. The magnitude of polarization-like modulation in the

¹¹This is a conservative estimate, as we have assumed the fractional systematic uncertainty in the 12 individual θ bins is equal to that of the average value of μ ; the fractional uncertainty in the individual bins should be larger than that of the average value, by a factor of $\sqrt{12}$ if they are Gaussian distributed.

lightcurve is $p < 0.041$ (90% confidence). This corresponds to an upper-limit on the intrinsic polarization of GRB 021206 of $\Pi < 214\%$; that is, we find that the analysis is insensitive to polarization at any level in GRB 021206.

The discrepancy between our derived upper-limit and the claimed detection by CB03 is due to two effects. First, during *detection*, CB03 neglected the systematic uncertainty in their null lightcurve, due to the Monte Carlo simulation of radiative transfer through the *RHESSI* mass model; the magnitude of this uncertainty is consistent with the magnitude of the observed modulation. In comparison, this systematic uncertainty does not play a role in the present $R(\theta)$ analysis, since the mass model is unnecessary. We are instead limited by Poisson noise. Thus, we conclude that the modulation interpreted as due to polarization by CB03 is instead due to systematic uncertainty in their null lightcurve.

Second, during *correction* of the detection of polarization signals into the magnitude of intrinsic polarization in GRB 021206 we find $11 \pm 3\%$ of all detected double-count events in our selection are due to scattering events. This results in a low signal-to-noise ratio, and a resulting high upper-limit on Π , such that the observation does not constrain the intrinsic polarization of GRB 021206. We justified our data selections and demonstrate that the signal should be clean of irreducible background. In contrast, CB03 estimated that $66 \pm 1\%$ of their detected double-count events were due to scattering events, while not describing or justifying their selection criteria. Specifically, our duplication of the analysis of CB03 found an unjustifiably larger “simultaneous” window ($\Delta T = 8$ b μ s, vs. $\Delta T = 5$ b μ s we used) and included the multi-count events (“bunches”) – both of which increase the background.

In our analysis, the limiting sensitivity is the highest theoretically possible – set by photon counting statistics. We therefore believe our analysis is more robust, and we conclude that: (1) the *RHESSI* observation of GRB 021206 is not sensitive to polarization, and (2) there is otherwise no evidence for polarization in the data.

In conclusion, we find that there is no existing constraint on the intrinsic polarization in the gamma-ray flux of GRB 021206 – or, for that matter, any gamma-ray burst. It seems unlikely that a constraint will emerge from further *RHESSI* observations. GRB 021206 was extremely bright (brighter than any GRB observed during 8 years of full-sky coverage with ULYSSES; Atteia et al. 1999) and detector deadtime already played a role in decreasing the signal-to-noise ratio at the peak of the burst, meaning an even brighter burst will only moderately improve the signal-to-noise ratio; also, GRB 021206 was located within 5% of the sky closest to the solar limb, as it must to take advantage of the polarization detection approach used herein (distinctly different from that used to measure polarization in solar flares McConnell et al. 2002), further decreasing the likelihood of a useful constraint on GRB polarization with *RHESSI*. Such a measurement must therefore wait for more

sensitive instrumentation.

We thank David Smith (UC Santa Cruz) for discussions regarding the *RHESSI* mass model, and for useful conversations about the *RHESSI* spectrometer detectors, contributions to double-count event backgrounds and data analysis; Wayne Coburn and Steve Boggs for detailed conversations about their approach and conclusions; and Andrew MacFadyen for comments on the manuscript. We are grateful to Gordon Hurford for detailed description and software to produce the roll-angle solution for *RHESSI* at the time of the gamma-ray burst. We acknowledge useful comments by the anonymous referee which encouraged us to attempt to reproduce the results of CB03.

References

- Atteia, J.-L. and Boër, M. and Hurley, K., 1999, *A&AS* 138, 421
- Bloom, J. S., Kulkarni, S. R., & Djorgovski, S. G., 2002a, *AJ* 123, 1111
- Bloom, J. S., Kulkarni, S. R., Djorgovski, S. G., Eichelberger, A. C., Cote, P., Blakeslee, J. P., Odewahn, S. C., Harrison, F. A., Frail, D. A., Filippenko, A. V., Leonard, D. C., Riess, A. G., Spinrad, H., Stern, D., Bunker, A., Dey, A., Grossan, B., Perlmutter, S., Knop, R. A., Hook, I. M., & Feroci, M., 1999, *Nature* 401, 453
- Bloom, J. S., Kulkarni, S. R., Price, P. A., Reichart, D., Galama, T. J., Schmidt, B. P., Frail, D. A., Berger, E., McCarthy, P. J., Chevalier, R. A., Wheeler, J. C., Halpern, J. P., Fox, D. W., Djorgovski, S. G., Harrison, F. A., Sari, R., Axelrod, T. S., Kimble, R. A., Holtzman, J., Hurley, K., Frontera, F., Piro, L., & Costa, E., 2002b, *ApJ* 572, L45
- Bloser, P. F., Hunter, S. D., Depaola, G. O., & Longo, F., 2003, in *Proc. SPIE Vol. 5165, "X-ray and Gamma-Ray Instrumentation for Astronomy XIII"*, astro-ph/0308331
- Coburn, W. & Boggs, S. E., 2003, *Nature* 423, 415
- Eichler, D. & Levinson, A., 2003, *ApJ* 596, 147
- Frail, D. A., 2003, *GRB Circular Network* 2280
- Granot, J., 2003, *ApJ*, in press, astro-ph/0306322
- Hjorth, J., Sollerman, J., Møller, P., Fynbo, J. P. U., Woosley, S. E., Kouveliotou, C., Tanvir, N. R., Greiner, J., Andersen, M. I., Castro-Tirado, A. J., Castro Cerón, J. M., Fruchter, A. S., Gorosabel, J., Jakobsson, P., Kaper, L., Klose, S., Masetti, N., Pedersen, H., Pedersen, K., Pian, E., Palazzi, E., Rhoads, J. E., Rol, E., van den Heuvel, E. P. J., Vreeswijk, P. M., Watson, D., & Wijers, R. A. M. J., 2003, *Nature* 423, 847
- Hurley, K., Cline, T., Smith, D. M., Lin, R. P., McTiernan, J., Schwartz, R., Wigger, C., Hajdas, W., Zehnder, A., Mitrofanov, I., Charyshnikov, S., Grinkov, V., Kozyrev, A.,

- Litvak, M., Sanin, A., Boynton, W., Fellows, C., Harshman, K., Shinohara, C., Starr, R., Mazets, E., Golenetskii, S., von Kienlin, A., Lichti, G., & Rau, A., 2003, *GRB Circular Network* 2281, 1
- Lazzati, D., Rossi, E., Ghisellini, G., & Rees, M. J., 2003, *a*
- Lin, R. P., Dennis, B. R., Hurford, G. J., Smith, D. M., Zehnder, A., Harvey, P. R., Curtis, D. W., Pankow, D., Turin, P., Bester, M., Csillaghy, A., Lewis, M., Madden, N., van Beek, H. F., Appleby, M., Raudorf, T., McTiernan, J., Ramaty, R., Schmahl, E., Schwartz, R., Krucker, S., Abiad, R., Quinn, T., Berg, P., Hashii, M., Sterling, R., Jackson, R., Pratt, R., Campbell, R. D., Malone, D., Landis, D., Barrington-Leigh, C. P., Slassi-Sennou, S., Cork, C., Clark, D., Amato, D., Orwig, L., Boyle, R., Banks, I. S., Shirey, K., Tolbert, A. K., Zarro, D., Snow, F., Thomsen, K., Henneck, R., Mchedlishvili, A., Ming, P., Fivian, M., Jordan, J., Wanner, R., Crubb, J., Preble, J., Matranga, M., Benz, A., Hudson, H., Canfield, R. C., Holman, G. D., Crannell, C., Kosugi, T., Emslie, A. G., Vilmer, N., Brown, J. C., Johns-Krull, C., Aschwanden, M., Metcalf, T., & Conway, A., 2002, *Sol. Phys.* 210, 3
- Lyutikov, M., Pariev, V. I., & Blandford, R. D., 2003, *ApJ*, submitted, astro-ph/0305410
- Matsumiya, M. & Ioka, K., 2003, *ApJ* 595, L25
- McConnell, M. L., Ryan, J. M., Smith, D. M., Lin, R. P., & Emslie, A. G., 2002, *Sol. Phys.* 210, 125
- Nakar, E., Piran, T., & Waxman, E., 2003, astro-ph/03407290
- Smith, D. M., 1998, *MNRAS* 301
- Smith, D. M., Lin, R. P., Turin, P., Curtis, D. W., Primbsch, J. H., Campbell, R. D., Abiad, R., Schroeder, P., Cork, C. P., Hull, E. L., Landis, D. A., Madden, N. W., Malone, D., Pehl, R. H., Raudorf, T., Sangsingkeow, P., Boyle, R., Banks, I. S., Shirey, K., & Schwartz, R., 2002, *Sol. Phys.* 210, 33
- Stanek, K. Z., Matheson, T., Garnavich, P. M., Martini, P., Berlind, P., Caldwell, N., Challis, P., Brown, W. R., Schild, R., Krisciunas, K., Calkins, M. L., Lee, J. C., Hathi, N., Jansen, R. A., Windhorst, R., Echevarria, L., Eisenstein, D. J., Pindor, B., Olszewski, E. W., Harding, P., Holland, S. T., & Bersier, D., 2003, *ApJ* 591, L17

Fig. 1.— Diagram of *RHESSI* spectrometer detector layout. Each circle represents the 7.1 cm diameter detector unit. The numbering of the detectors corresponds to that in general use, and these are shown as from the solar perspective. The sense of rotation shown is the rotation of the spacecraft; the axis of rotation is not that shown, but is instead close to the coordinate origin, (0,0).

Fig. 2.— **(a)** Histogram of time-stamp separation of consecutive counts in GRB 021206, in units of 2^{-20} s (μs). **(b)** Same as (a), except consecutive counts in the same detector have been replaced by a single count at the earlier timestamp. The peak at non-zero value of ΔT indicates that simultaneous counts can have time-stamps which are not equal. We thus adopt the convention that counts with timestamps which differ by ≤ 5 μs are “simultaneous”.

Fig. 3.— The 0.15-2.0 MeV lightcurve of GRB021206, as observed with *RHESSI*, beginning at 2002 Dec 6 22:49:10 UT. The two vertical lines delineate the 5.0s period used in the present analysis, which were chosen to match the analysed data in CB03.

Fig. 4.— Relative frequency of double-count events, by detector. Top panel: Data points, with error bars, give the number of double-count events associated with each detector and their Poissonian uncertainties. The solid histogram represents the best-fit scattering + coincidence model to these data, which has $11 \pm 3\%$ scattering. Dotted histograms show the contributions of scattering (lower histogram) and coincidence (upper histogram), respectively. Bottom panel: Residuals of the data compared to the model, scaled to the Poisson uncertainties. All double-events that interact with detector 2 have been excluded from this analysis; see text for details.

Fig. 5.— In these figures, $\theta = 0$ and $\theta_n = 0$ correspond to celestial north, with increasing value rotating east of north about the detector origin (clockwise, facing the Sun; cf. Fig 1). The position of GRB 021206 is marked in each panel by a vertical broken line. **(a)** Single event countrate S as a function θ , where θ is the angle between celestial north and the center of the detector in which the count is observed, in the range 0-360 deg. The countrate is inconsistent with being constant in θ , with the χ^2_ν shown, and a probability of observing such variability of $< 10^{-100}$. **(b)** Double-count event countrate D as a function of θ ; here, we place 1 count for each of the two involved in the event, with each being placed in the appropriate θ bin. The strong variability is inconsistent with being constant in θ , with the given χ^2_ν , and a probability of of observing such variability of $< 10^{-50}$. **(c)** The ratio S/D is consistent with being constant (prob=0.54). **(d)** The single-count event rate S in our polarization analysis, as a function of sky angle θ_n in the range 0-180 deg (see §4). The countrate is inconsistent with being constant in θ_n . **(e)** The double-count event rate D in our polarization analysis, as a function of sky angle θ_n , which has values in the range 0-180 deg (see §4). This figure is

directly comparable to the double-count event rate of CB03, without having subtracted the Monte Carlo “null” lightcurve. As in CB03, we also find significant variability as a function of θ_n . **(f)** The ratio $R = D(\theta_n)/S(\theta_n)$ vs. sky angle θ_n . Polarized photons would scatter through a preferred angle on the sky, producing more double-count events in that direction relative to single count events than in the perpendicular direction, producing variation in $R(\theta_n)$. However, R is observationally consistent with being constant in θ ; thus, we find no evidence of polarization.

Fig. 6.— **Panel a:** The relative Klein-Nishina cross-section for a pair of detectors as a function of angle between the initial photon direction and a line between the two detectors, at four different photon energies (listed top to bottom). **Panel b:** The relative cross section for a double-scatter event for a pair of detectors due to the Klein-Nishina cross section, as a function of angle between the detectors and the direction of the GRB projected in the plane of the detectors, assuming the GRB is offset by 18 deg from the axis of the plane occupied by the detectors (zero offset would produce zero modulation). At 18 deg, the magnitude of modulation is between 7% (for 0.15 MeV photons) and 9.5% (for 2.0 MeV photons). The solid lines are for the same photon energies as given in panel a, with larger energies producing greater variation. The dotted line is the $I(\theta)$ pattern *only* for a polarized photon beam, with $p = 0.045$ and $\theta_p = 0$. **Panel c:** The inferred fractional polarization due only to the K-N cross-section, as a function of photon energy.

Fig. 7.— **a)** Data copied from Fig.2 of CB03. (Top Panel) Crosses are the double-count event lightcurve $D(\theta)$ as a function of angle on the sky θ . Solid squares are the MC-simulated null-lightcurve $D_{\text{null}}(\theta)$. Note the data is repeated at 180 deg. (Bottom Panel) Residual counts, $D(\theta) - D_{\text{null}}(\theta)$, exhibiting the modulation in θ interpreted by CB03 as due to polarization in GRB 021206. The solid-line is their best-fit of a polarization signal (also in panels b and d). **b)** (Top Panel) Our duplication of the results of CB03, finding data selections which reproduce their $D(\theta)$ (see text), with symbols having the same meaning as in panel a. The solid points, however, are the $D_{\text{null}}(\theta)$ values calculated by CB03, renormalized (see text). (Bottom Panel) The residual counts curve duplicates well that of CB03. **c)** The ratio $R(\theta) = D(\theta)/S(\theta)$, using our duplicate data selection. The sinusoidal modulation in $D(\theta) - D_{\text{null}}(\theta)$ is not present in $R(\theta)$; instead, the ratio shows significant random scatter. **d)** The same analysis as in panel b, but with the multi-count events removed from the dataset. The modulation in $D(\theta) - D_{\text{null}}(\theta)$ is reduced, but still present. **e)** The ratio $R(\theta)$ using the same data set as panel d. The scatter in panel (c) has disappeared (due to the multi-count events removed), and no modulation is present. This implies that $D(\theta) \propto S(\theta)$ and that the modulation in $D(\theta) - D_{\text{null}}(\theta)$ seen by CB03 (panel a), and duplicated here in panels b and c, is not due to polarization-related modulation in $D(\theta)$, but in $D_{\text{null}}(\theta)$ (the null lightcurve).

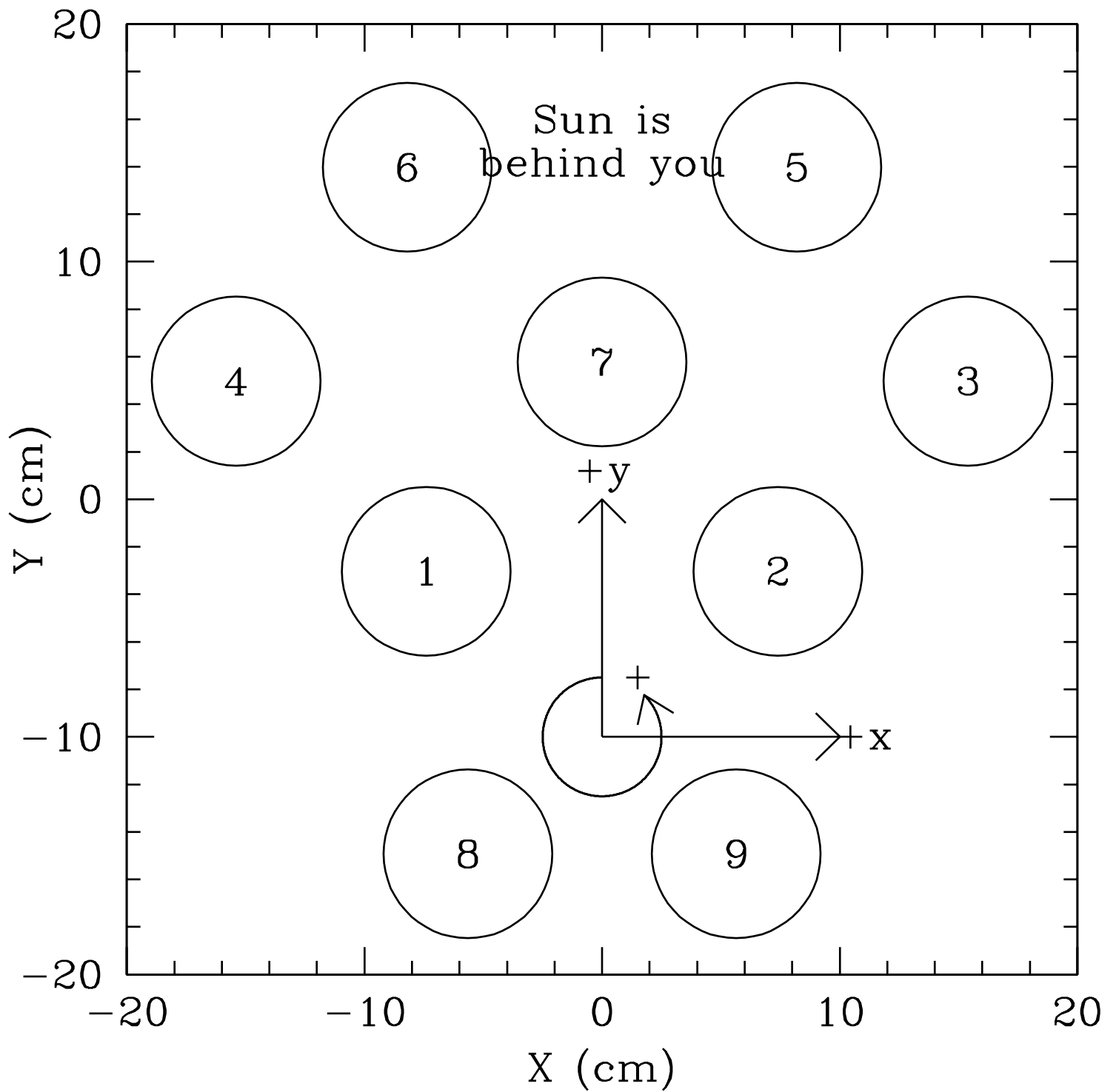


Figure 1

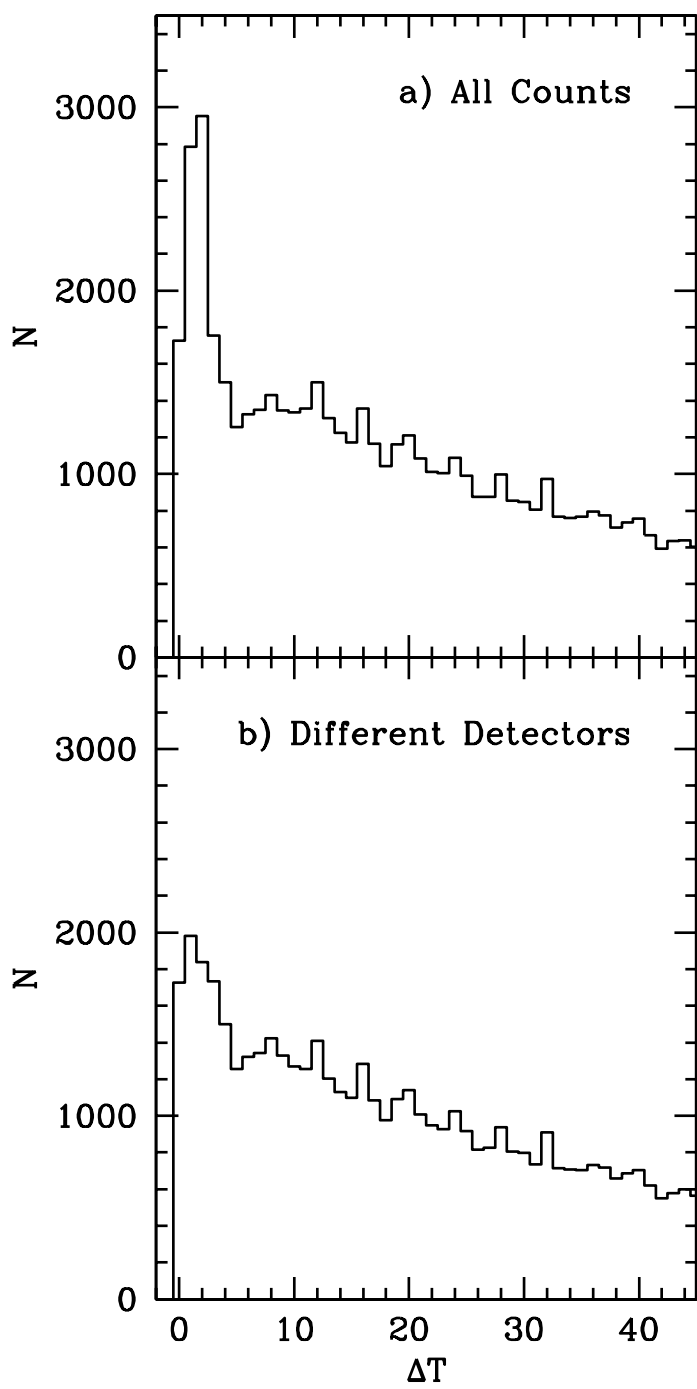


Figure 2

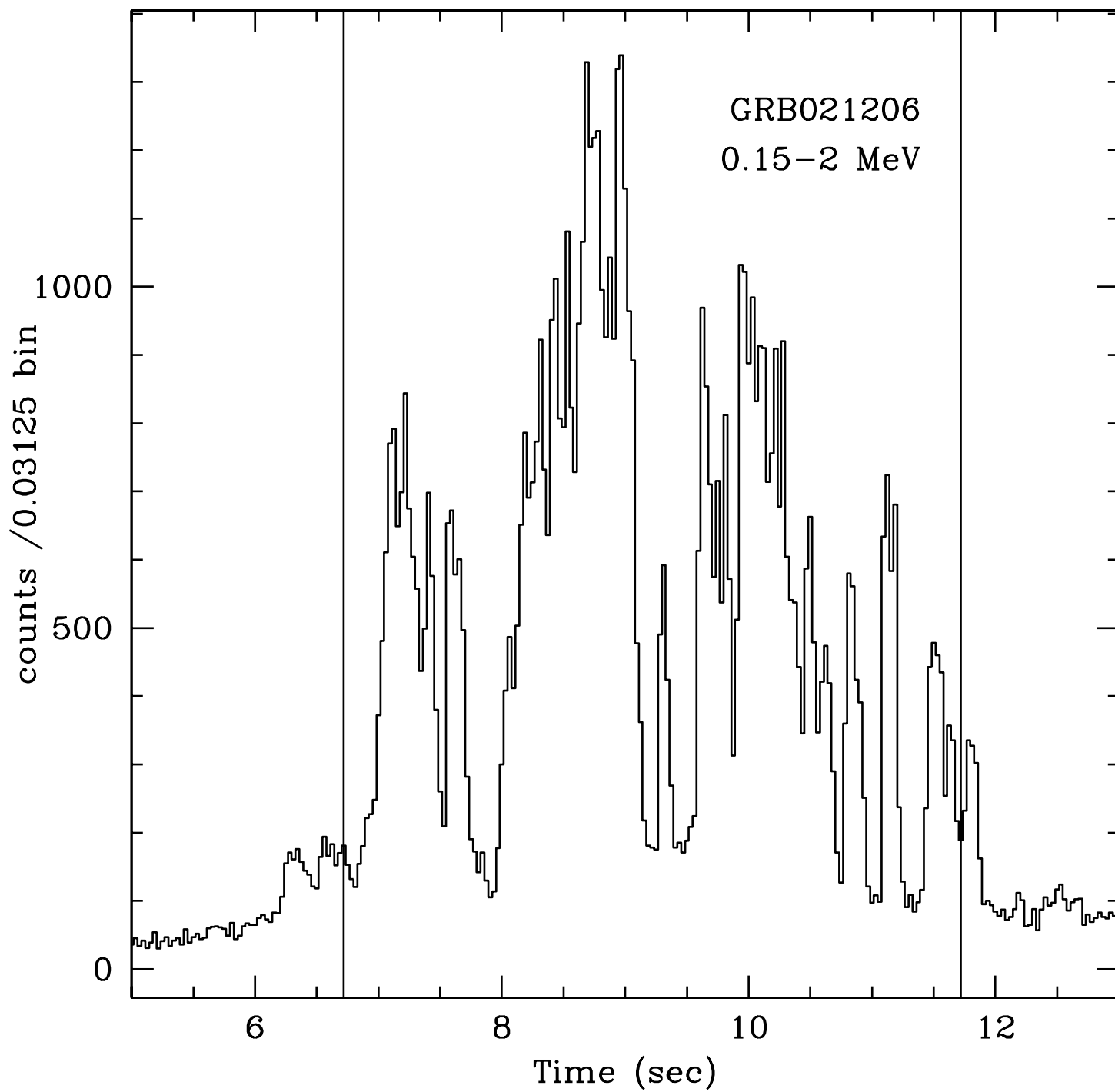


Figure 3

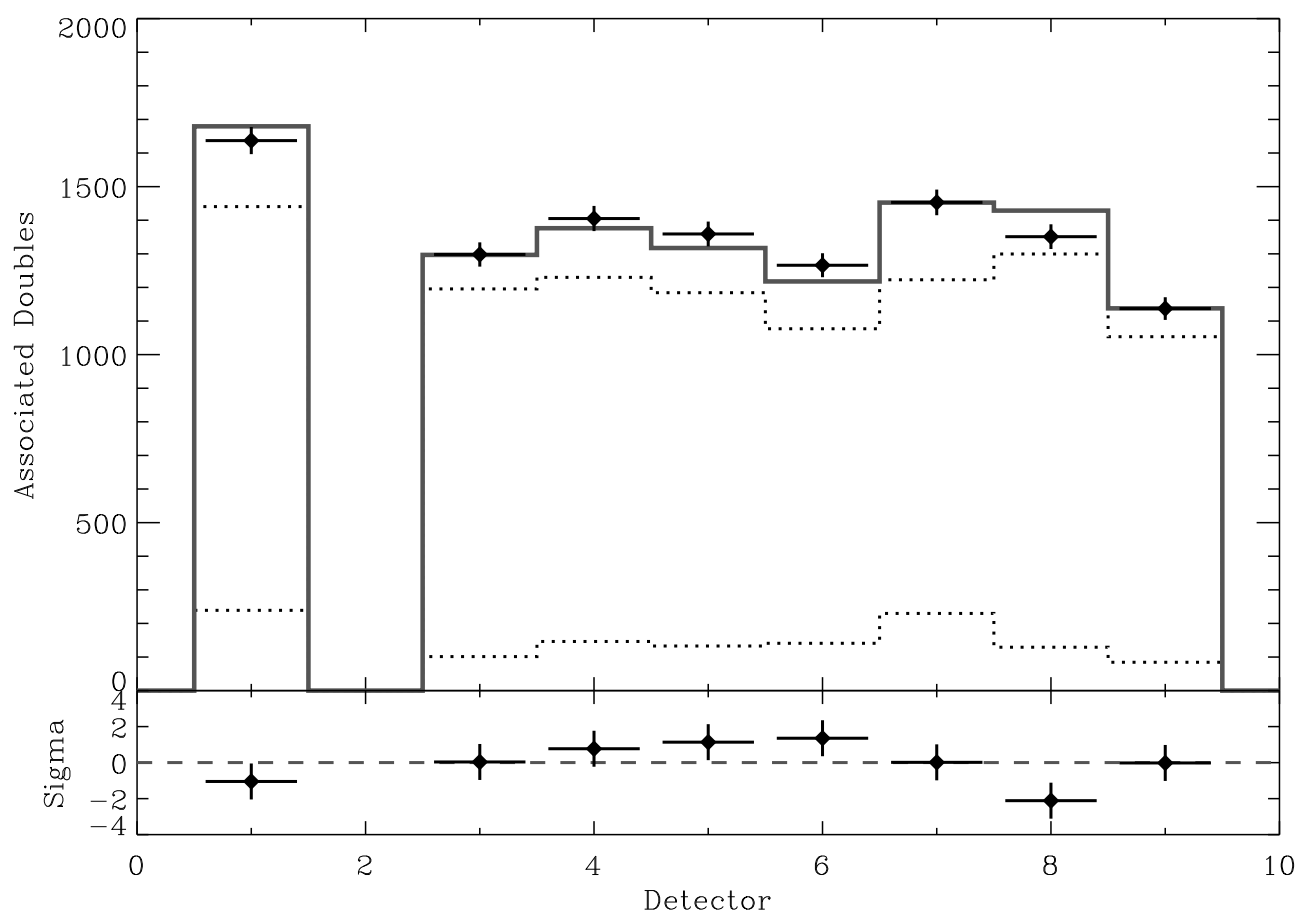


Figure 4

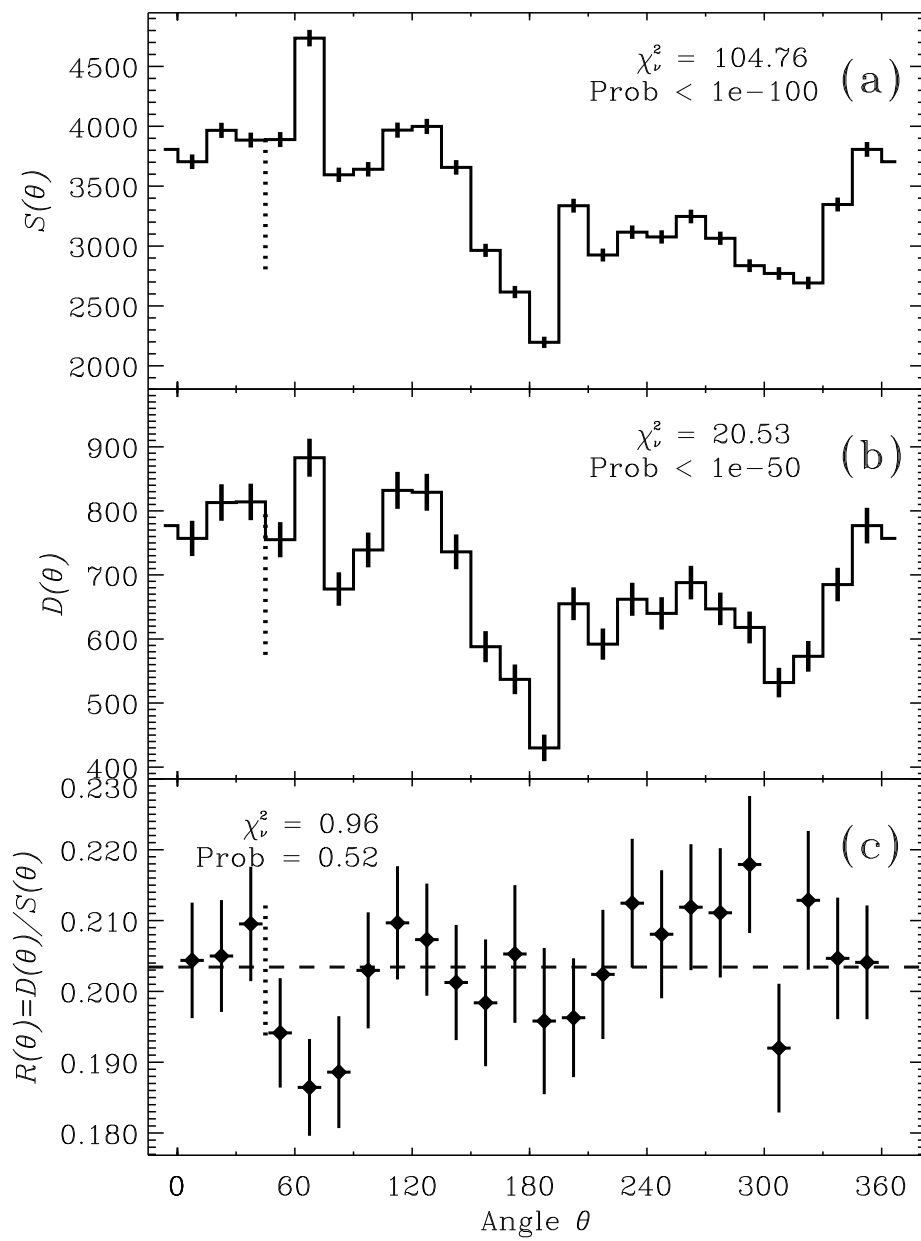


Figure 5a-c

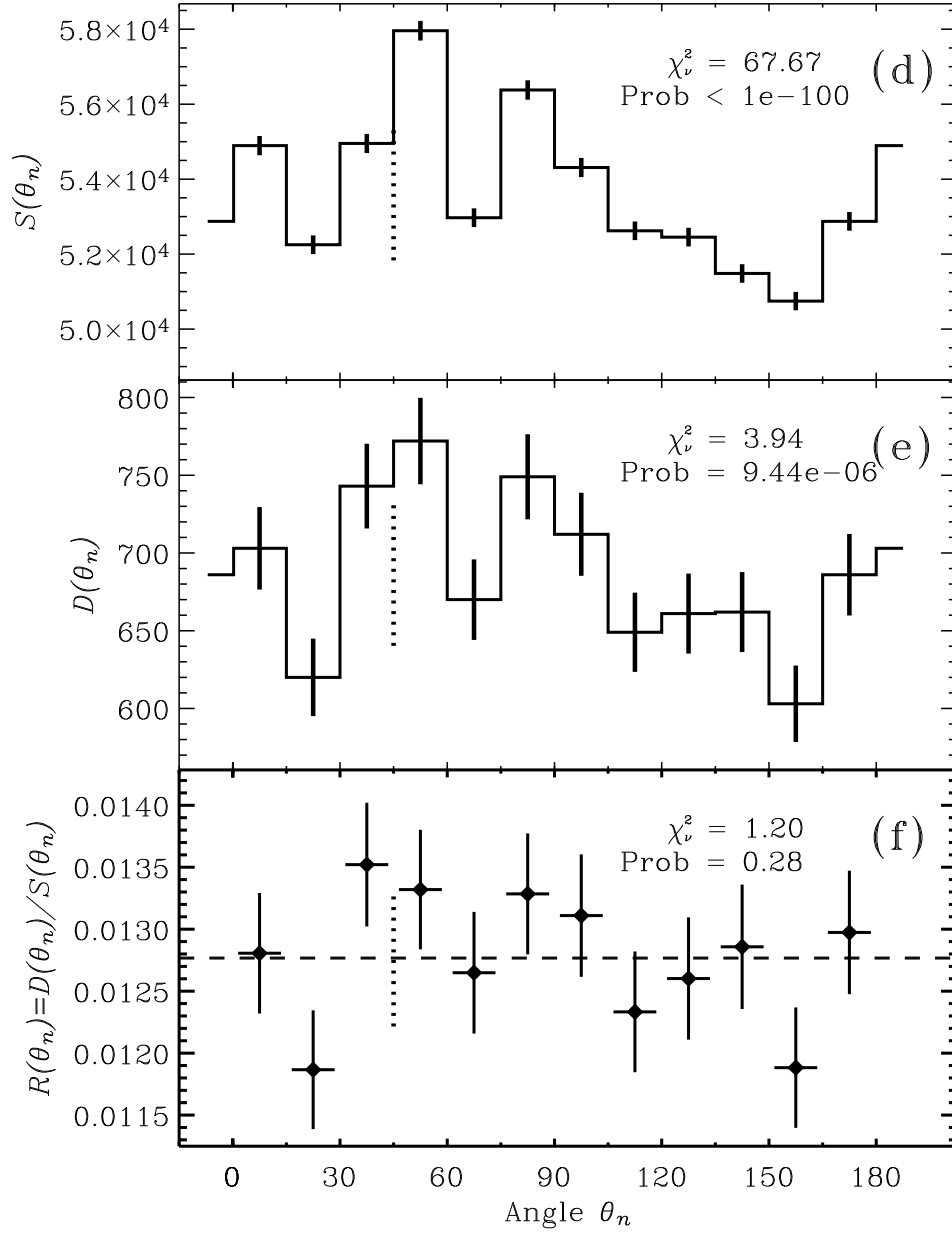


Figure 5d-f

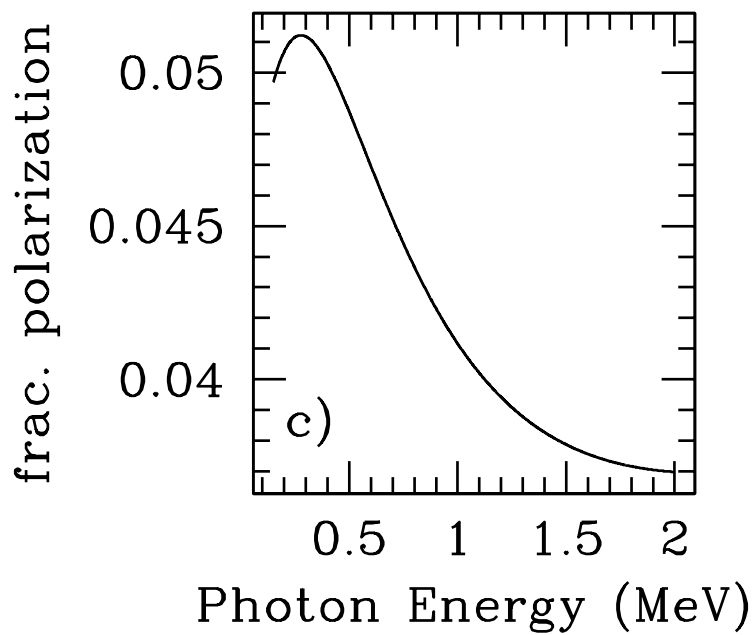
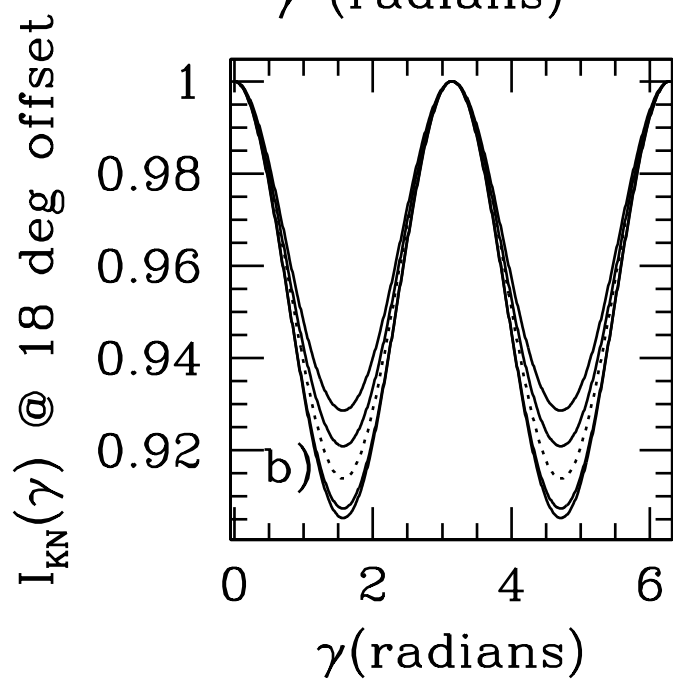
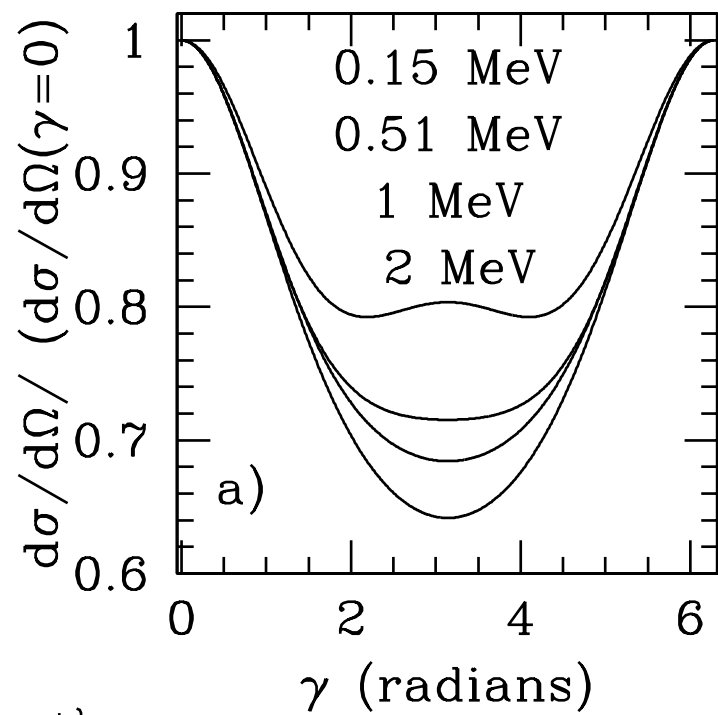


Figure 6

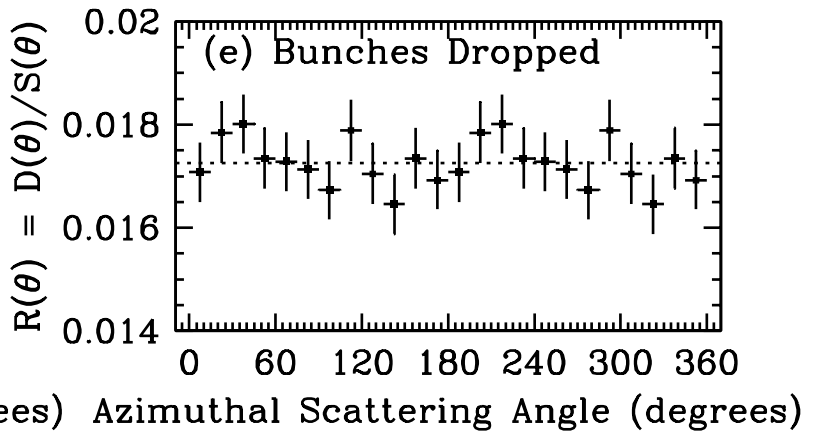
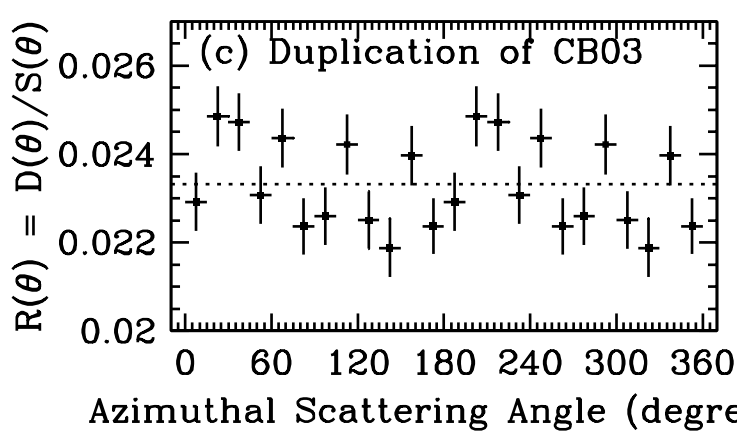
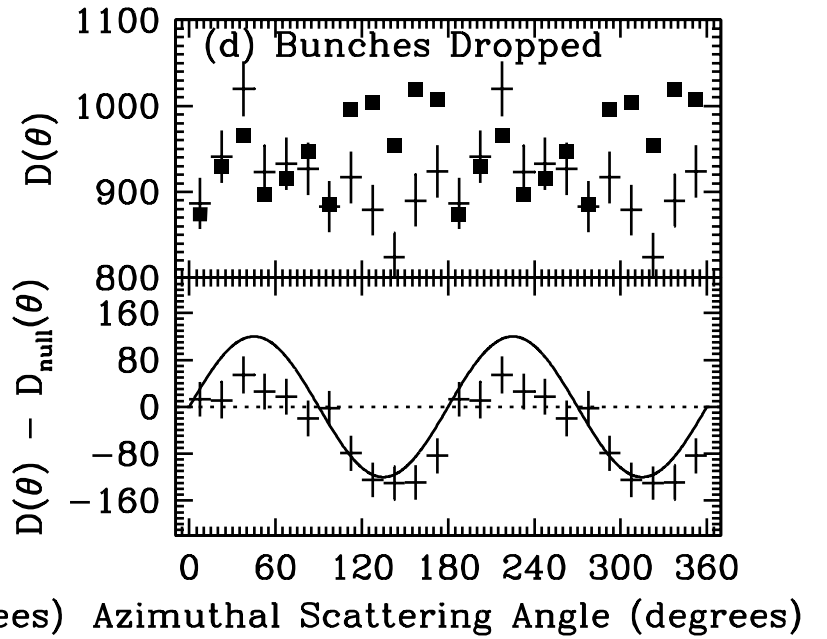
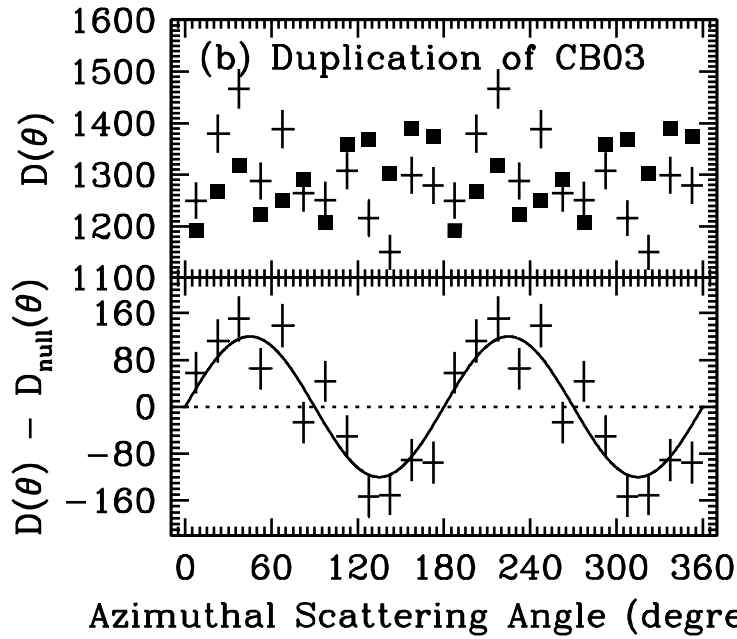
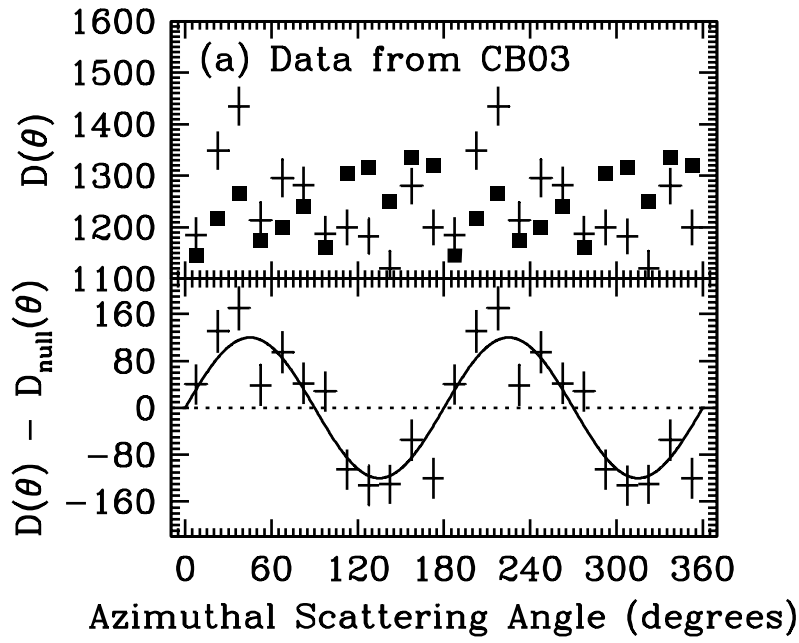


Figure 7

Table 1. Detector Physical Parameters

Detector #	X (cm)	Y (cm)	Ω_i (relative solid angle)	I_i (counts)
1	-7.4	-3.0	3.73	9870
2	7.4	-3.0	n/a	n/a
3	15.4	5.0	1.90	8191
4	-15.4	5.0	2.68	8426
5	8.2	14.0	2.52	8114
6	-8.2	14.0	2.94	7379
7	0.0	5.8	4.23	8377
8	-5.6	-14.9	2.24	8903
9	5.6	-14.9	1.80	7216

Table 2. Double-Count Events and Irreducible Background

Events	Present work	CB03
Total Double-Count Events Found	8230	14916
Coincidences	6640 \pm 80	4488 \pm 72
Other Background ^a	760 \pm 110	588 \pm 25
Double-Count Scattering Events ^b	830 \pm 150	9840 \pm 96

Note. — ^aIn the present work this is the background due to the “unknown” mechanism. In CB03, this is the value labeled “background scatters”. ^bUsing a second, independent method which does not require detailed examination of the different background contributions, we find 910 \pm 250 two-detector scattering events, which lends us confidence in this value. See §2.5.